

A SILICON/SOLDER BILAYER THERMAL ACTUATOR FOR COMPENSATING THERMAL DRIFT OF SILICON SUSPENSIONS

Huafeng Liu and W. T. Pike

Optical and Semiconductor Devices Group, Imperial College London, London, UK

ABSTRACT

We introduce a novel thermal compensation scheme to passively compensate the temperature coefficient of Young's modulus with a thermal actuator using solder encapsulated by silicon cavities. Our approach produces a silicon/solder bilayer within the base of a suspension to effect an angular strain deflecting the proof mass supported by the suspension. A proof-of-principle thermal actuator has been fabricated. Temperature cycling experiments give a good agreement with both closed form and FEA models. We apply this technique to produce a thermally compensated low-frequency vertical microseismometer, without affecting the mechanical and electrical properties of the suspension. Using this approach we demonstrate the thermal coefficient of a vertical suspension is reduced from -60 ppm to less than 1 ppm/C.

KEYWORDS

Temperature Compensation, Thermal Actuator, Drift, Solder Reflow, Micro-fabrication, Seismometer

INTRODUCTION

It is well known that resonating silicon sensors suffer from the temperature-dependent elasticity of their flexures [1]. As temperature varies, there is a shift of the resonant frequency due to the suspension stiffness change. There are a number of techniques to compensate for this effect. Active approaches include packaging in temperature-stabilized micro-ovens [2] or bias-current tuning [3], both requiring extra control electronics and devices. Passive approaches use composite materials in the springs, for example substrate doping [4, 5] and oxide-refilled trenches [6]. However, the introduction of additional materials affects the device damping as well as the electrical characteristics of the beam.

A particular example of this effect relates to the use of flexures to support the proof mass of an accelerometer in the presence of the gravitational field of the Earth. The vertical axis of an accelerometer will experience a temperature-dependent sag equal to the gravitational acceleration divided by the square of the resonant angular frequency. For instance, a 10-Hz accelerometer will sag 2.5mm under gravity and drift 1.5 μ m over 10C due to the temperature coefficient of Young's modulus of silicon, compromising accurate sensing of the proof mass position. Compared with frequency-based resonators, the challenge of improving the determination of the proof-mass displacement in accelerometers is not primarily to stabilize the resonant frequency, but to compensate the variation of the thermally

induced sag that can dominate the measurement.

None of the existing methods can meet this challenge without using extra circuits and sensors, or affecting the mechanical and electrical characteristics of the suspension. Hence, we have developed a passive approach that uses thermal actuation to tilt the suspension support rather than affects the suspension itself.

APPROACH

The basis of our compensation approach is to use the thermally induced deflection of a bilayer structure at the base of the suspension to produce an angular strain (see fig.1). As the temperature is elevated, the proof mass of the seismometer is lifted up by the angular strain induced by the compensator structures at the same time as the softening of the suspension causes the proof mass to drop under gravity. The overall effect should be designed to minimize motion of the proof mass due to temperature.

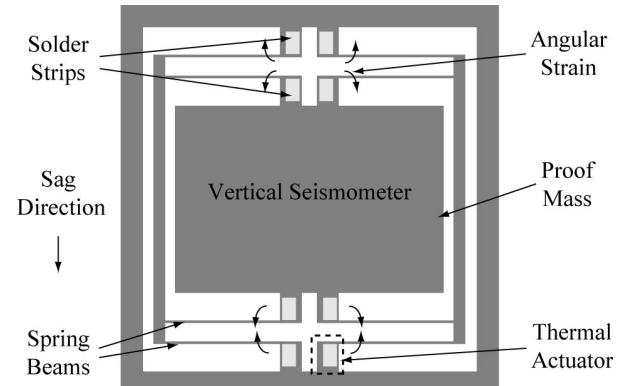


Figure 1: Illustration of temperature compensation for a vertical microseismometer with eight thermal actuators at the bases of the silicon suspension.

A simplified geometry illustrates the angular strain needed to compensate for the thermal variation of the sag (fig.2). The displacement of the proof mass can be derived according to Hook's law:

$$x = x_0 + x(T) = \frac{mg}{k(T)} = \frac{4mgL^3(T)}{E(T)w(T)t^3(T)} \quad (1)$$

where x_0 is the sag at the temperature selected for compensation, with E , Young's Modulus and L , w , t , the length, width and thickness of the cantilever, all temperature dependent. Assuming isotropic elasticity and linear thermal coefficients, the thermal dependence of the sag displacement will be

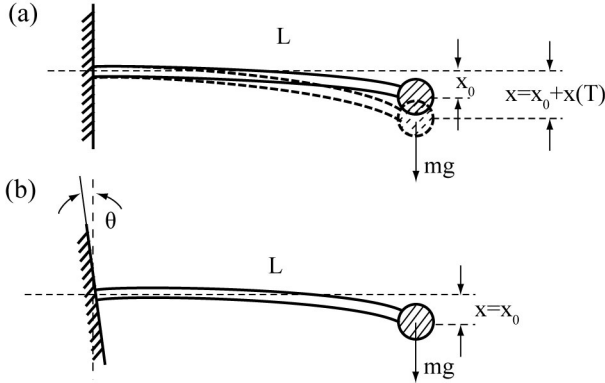


Figure 2: (a) Proof mass suspended by a cantilever under gravity; (b) proof mass lifted up by tilting the base of the cantilever.

$$\begin{aligned} \frac{\partial x_0}{\partial T} &= -x_0 \left(\frac{1}{E} \frac{\partial E}{\partial T} + \frac{1}{L} \frac{\partial L}{\partial T} \right) . \\ &= -x_0 (\alpha_E + \alpha_L) \end{aligned} \quad (2)$$

While composite materials can be used to make α_E and α_L equal and opposite, fig. 2b shows that by tilting the base of the cantilever this thermally induced sag can be compensated without changing the suspension materials. In this case the total sag will be

$$x = \frac{mg}{k(T)} - L(T)\theta(T) \quad (3)$$

giving

$$\begin{aligned} \frac{\partial x}{\partial T} &= -x_0 (\alpha_E + \alpha_L) - L \left(\theta \alpha_L + \frac{\partial \theta}{\partial T} \right) \\ &= -x_0 (\alpha_E + \alpha_L) - L \frac{\partial \theta}{\partial T} \end{aligned} \quad (4)$$

as the tilt θ will always be a small angle to the horizontal such that $L\theta \ll x_0$. Hence thermal compensation will be achieved if $\partial\theta/\partial T = 0$; therefore, the requested tilt angle against temperature can be derived in (5).

$$\frac{\partial \theta}{\partial T} = -\frac{x_0}{L} (\alpha_E + \alpha_L) . \quad (5)$$

DESIGN AND FABRICATION

To effect this tilt solder, with a larger coefficient of thermal expansion than silicon, is introduced into the base of the suspension to produce an effective bilayer strip (see fig.3). However, the ability of the bilayer to thermally bend is dependent on maintaining a bond at the solder-silicon interface and this thermally induced interfacial stress can easily break the inherently weak bonding between the two materials. Hence our structure contains shaped cavities to ensure as the solder is cooled from melting, it produce a strong shrink fit bond to the silicon. These cavities are etched at the base of the suspension during the through-wafer deep reactive-ion etch (DRIE) used to form the

suspension. The fabrication processes are based on a single mask. Firstly, an aluminum layer was evaporated on the backside of a silicon wafer to alleviate notching during through-wafer etching. After features transferred by lithography, the wafer was loaded into DRIE for the first etching run. Then, a backing wafer was attached to the backside to hold the devices for further etching. Photoresist and aluminum were striped by acetone and the etching solution respectively. Devices were singulated by breaking the small tabs connected on the devices (dicing-free).

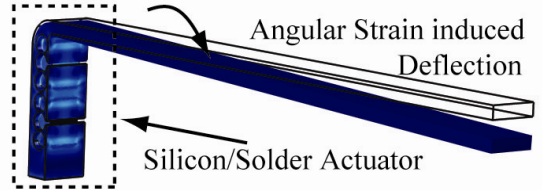


Figure 3: A proof-of-principle design of a silicon/solder thermal actuator having an angular strain induced deflection after solder reflow, simulated in COMSOL.

A simplified model that is amenable to closed-form solution, a more complex FEA model and the as-fabricated thermal actuator are illustrated in fig.4.

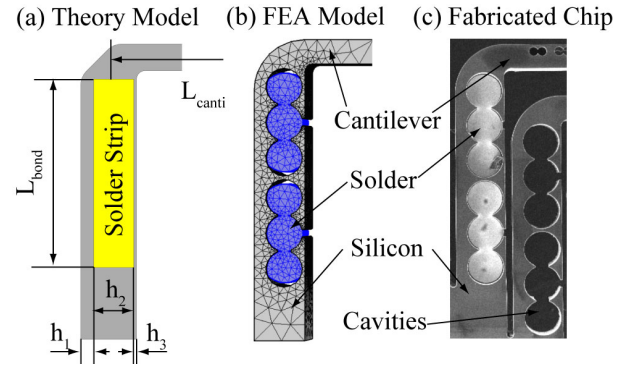


Figure 4: Thermal actuator models and a fabricated chip (actuator bases are anchored).

Considering the thermal compensator as a trilayer a closed-form solution for the temperature coefficient of curvature, f ,

$$\frac{1}{r} = f(E_i, h_i, \alpha_i) \cdot \Delta T \quad (6)$$

is given in [7] where E_i , h_i and α_i are Young's Moduli, thickness and CTEs respectively of each layer and the subscripts 1, 2, 3 represent the thicker silicon layer, the solder layer and the thinner silicon layer respectively.

As the angular strain only occurs at the bonding area, the tilt angle of the thermal actuator depends on the effective bonding length L_{bond} . Hence, the thermal tilt of a thermal actuator can be derived as

$$\frac{\Delta \theta}{\Delta T} = \frac{L_{bond}}{r} \frac{1}{\Delta T} = f(E_i, h_i, \alpha_i) L_{bond} . \quad (7)$$

To fully compensate the suspension, it is hence necessary for

$$f(E_i, h_i, \alpha_i) L_{bond} = -\frac{x_0}{L}(\alpha_E + \alpha_L). \quad (8)$$

RESULTS

Proof-of-principle Demonstration Test

To verify the theoretical analysis, both FEA simulation and temperature cycling experiments of proof-of-principle chips were conducted. In fig.5, the thermal actuator (compensator) is at the base of a 7-mm long cantilever at

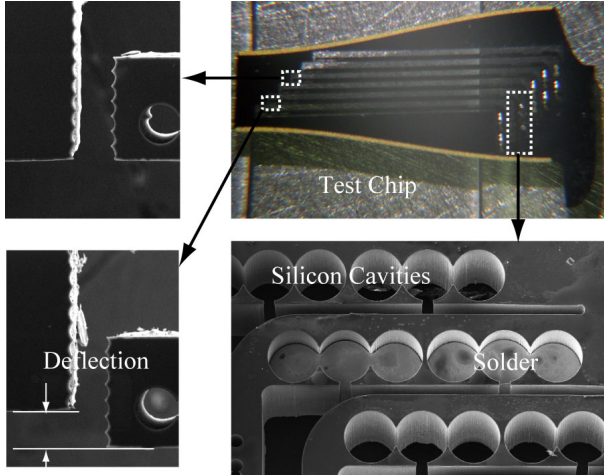


Figure 5: Proof-of-principle test chip (top right) showing that higher magnification of the elements of the compensator (lower right) and the thermally induced deflection.

whose distal end is an indicator moving against fiducials to measure the angular deflection induced by the compensator. Both SAC305 (3% silver 0.5% copper 96.5% tin) and AuSn (80% gold 20% tin) solder balls were used to fill the silicon cavities. According to the solder and silicon CTEs, Young's moduli, and the dimensions of the multilayer structure in Table.1, the angular deflection against temperature of the actuator can be calculated by (7) times with the cantilever length L_{canti} .

Table 1: Parameters of materials of each layer in the thermal actuator (SAC and AuSn are solder types).

Parameters	Silicon	SAC	AuSn
Young's modulus (GPa)	122	41	59.1
α_L (ppm/C)	2.6	23.5	16
Thickness (μm)	72/20	210	210
Reflow temperature (C)	-	220	280

Thermal cycling experiments were operated in a solder reflow rig. Testing chips were suspended at one side enabling cantilevers friction-free on the hotplate. The deflections against temperature of thermal actuators were recorded by a digital camera through the translational microscope above the reflow chamber. According to known

dimension references, the actual deflections were analyzed for each captured image.

The measured deflections over the cantilever length against temperature change have good agreement with both closed-form and FEA simulations results, shown in fig. 6. Thermal actuators loaded with SAC solder have a larger temperature coefficient than that with AuSn solder, since SAC has larger combined expansion effect from α_L and Young's Modulus than AuSn solder.

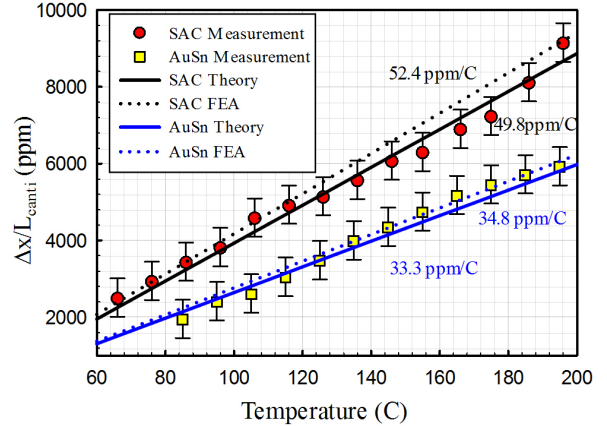


Figure 6: Comparison of temperature coefficients of thermal actuators using different solder materials (measurement data are normalized).

Seismometer Temperature Compensation Test

This temperature compensation approach is being applied to a silicon microseismometer that is going to be sent on Mars by NASA's InSight 2016 mission [8]. The fabricated seismometer with thermal compensators integrated is shown in fig. 7.

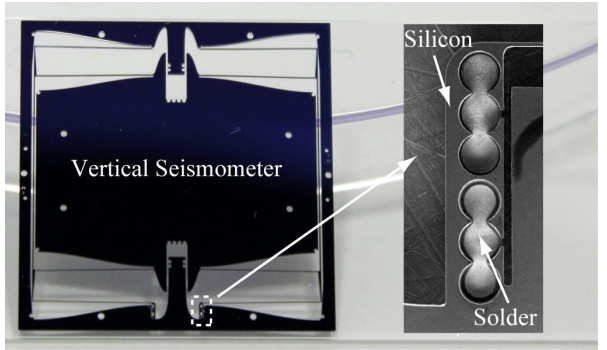


Figure 7: A fabricated vertical MEMS seismometer (20*20mm) with temperature compensators, tilted for operation under gravity.

The thermal drift compensation of this seismometer was tested as shown in fig. 8. The seismometer frame was fixed on a heater which was tilted with a certain angle to simulate the reduced effect of Martian gravity. A laser displacement transducer was aligned to position the laser spot on the proof mass of the seismometer, and the

reflection was sensed by a CMOS sensor inside the laser head. As the temperature was varied, the thermally induced motion of the proof mass was determined.

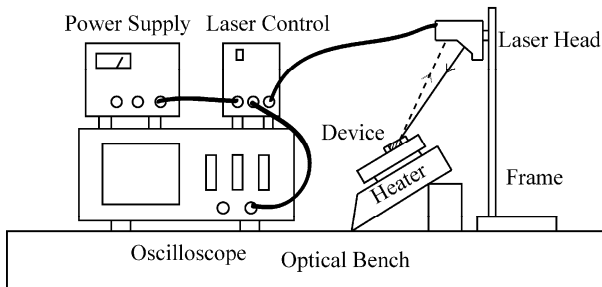


Figure 8: Testing setup to determine the thermal drift of a seismometer under gravity.

The displacement of the proof mass with and without compensation is plotted in fig.9 and again shows good agreement with both the closed-form and FEA simulation results. The introduction of the thermal actuators has reduced the temperature coefficient of the vertical axis of the seismometer displacement from around -60ppm/C to less than 1ppm/C.

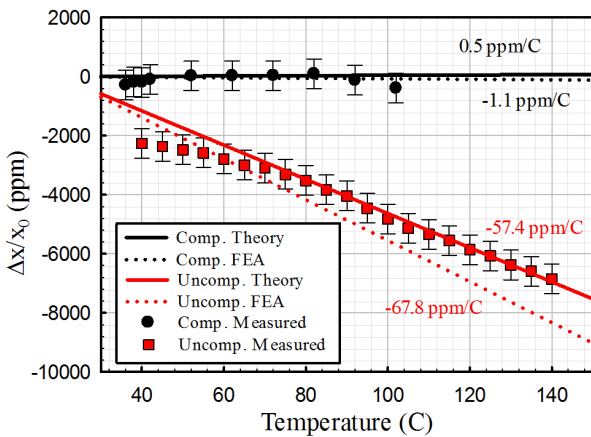


Figure 9: Comparison of the thermal sag drift of the seismometer with and without thermal compensation.

CONCLUSION

We have demonstrated that it is possible to compensate for the thermal drift of low-frequency suspensions subject to gravity, a response of particular concern to high-resolution acceleration measurements, using a thermal actuator to tilt the base of a suspension. Test results of the thermal compensator performance agree with both theoretical and FEA results. This thermal compensator has been applied to a vertical-axis silicon seismometer and the results demonstrate an attenuation of the thermal response by two orders of magnitude compared to the uncompensated device. Other applications of the thermal actuator developed in this work include thermometers and thermal switches.

ACKNOWLEDGEMENTS

We would like to thank Dr. Guangbin Dou, Dr. A. K. Delahunty and Dr. A. Mukherjee for devices fabrication.

REFERENCES

- [1] M. A. Hopcroft, W. D. Nix and T. W. Kenny, "What is the Young's Modulus of Silicon", *Journal of MEMS*, 19, 2 (2010).
- [2] J. C. Salvia, R. Melamud, S. A. Chandorkar, S. F. Lord, and T. W. Kenny, "Real-time temperature compensation of MEMS oscillators using an integrated micro-oven and a phase-locked loop", *Journal of MEMS*, 19, 1 (2010).
- [3] A. Hajjam, A. Logan, and S. Pourkamali, "Doping-Induced Temperature Compensation of Thermally Actuated High-Frequency Silicon Micromechanical Resonators", *Journal of MEMS*, 21, 3 (2012).
- [4] A. K. Samarao, and F. Ayazi, "Temperature Compensation of Silicon Resonators via Degenerate Doping", *IEEE Transactions on Electron Devices*, 59, 1 (2012).
- [5] M. Shahmohammadi, B. P. Harrington, and R. Abdolvand, "Zero temperature coefficient of frequency in extensional-mode highly doped silicon microresonators", *IEEE Frequency Control Symposium 2012*, Baltimore, MD, 21-24 May, 2012, pp.1-4.
- [6] M. Rais-Zadeh, V. A. Thakar, Zhengzheng Wu, and A. Peczalski, "Temperature compensated silicon resonators for space applications", *Proceedings of SPIE*, 8614, (2013) pp.86140E-86140E-7
- [7] H. Torun, and H. Urey, "Thermal deflections in multilayer microstructures and athermalization", *Journal of Applied Physics*, 100, 023527 (2006)
- [8] W. T. Pike, et. al, "A self-leveling nano-g silicon seismometer", *IEEE Sensors 2014*, Valencia, Spain, 2-5 Nov. 2014, pp. 1599-1602

CONTACT

*W. T. Pike, tel: +44 (0)20 7594 6207;
w.t.pike@imperial.ac.uk